Biomass Conversion and Biorefinery (2024) 14:11445–11457
https://doi.org/10.1007/s13399-022-03182-w

ORIGINAL ARTICLE

Realizing direct conversion of glucose to furfurals with tunable selectivity utilizing a carbon dot catalyst with dual acids controlled by a biphasic medium

Raina Sharma[1] · Abdul Selim[1] · Bhawana Devi[2,3] · Senthil M. Arumugam[2] · Shaifali Sartaliya[1] · Sasikumar Elumalai[2] · Govindasamy Jayamurugan[1]

Received: 25 May 2022 / Revised: 26 July 2022 / Accepted: 1 August 2022 / Published online: 10 August 2022

Abstract

Developing cost-effective processing strategies for the preparation of fuel-precursor chemicals, including 5-hydroxymethylfurfural (HMF) and furfural, has been dedicatedly researched over the last few years. These compounds are typically produced using different carbohydrate sources, say furfural using xylose and HMF using glucose. Herein, we report the significant formation of both these furfurals using a single glucose source over the fine-tuned **Fe^{2+}@SO_3-CD** nanocomposite. The catalyst exhibiting two different acidic sites, such as Lewis and Brønsted, developed by the iron (II) metal and sulfonate groups, respectively, offered a synergistic effect on the glucose decomposition into furfurals. Mechanistically, the iron (II) Lewis metal acid sites play a vital role in the significant formation of furfurals. Furthermore, the THF/H_2O biphasic system influenced a selective formation of HMF and furfural, achieving as high as 85% HMF (94% selectivity) in 1:2 THF/H_2O and 56% furfural (90% selectivity) in 1:1 THF/H_2O. The recyclability study showed that the catalyst is effective for 4 cycles. The green metrics analysis of the solid acid catalysis represented a greener strategy for furfurals production. Overall, the catalytic setup can be upscaled because of the involvement of cheaper precursors and less labor-intensive catalyst preparation.

Keywords Carbon dots · Lewis and Brønsted acids · Glucose · 5-hydroxymethylfurfural · Furfural · Biomass · Biphasic solvent

1 Introduction

Energy has become vital in modernization, globalization, and civilization [1]. Back in the late nineteenth century, fossil fuels were the sole source of energy [2]. Nowadays, the world is attempting to change away from a petroleum-based economy to a biomass-based one to get out of this predicament [3]. As a renewable and environmentally friendly source of organic carbon, biomass is one of the most promising sources today [4]. One of the interesting features of biomass is its carbohydrate content, which can be transformed into high-value-added materials or compounds, including polymers, fuels, fuel additives, chemicals, etc. [5–7]. 5-hydroxymethylfurfural (HMF) and furfural are identified as bio-based renewable platform chemicals that can be used to synthesize liquid fuels, pharmaceuticals, solvents, plastics, polymers, functional small molecules, *etc.* [8–11]. In conventional acidic (mineral) catalysis, glucose is converted to levulinic acid *via* a series of *in situ* reactions, including isomerization (to yield fructose), dehydration (to yield HMF), and rehydration (to yield levulinic acid) [5–7, 12–14]. Typically, HMF is produced using glucose, which can be derived from biomass *via* cellulose hydrolysis, whereas furfural uses xylose (which is a backbone sugar component of biomass hemicellulose) [15–17]. Based on the literature, organic polar aprotic solvents contribute to higher

✉ Sasikumar Elumalai
sasikumar@ciab.res.in

✉ Govindasamy Jayamurugan
jayamurugan@inst.ac.in

[1] Energy and Environment Unit, Institute of Nano Science and Technology, Knowledge City, Sector 81, SAS Nagar, Manauli PO, Mohali, Punjab 140306, India

[2] Chemical Engineering Division, DBT-Center of Innovative and Applied Bioprocessing, Knowledge City, Sector 81, Mohali, Punjab 140306, India

[3] Department of Chemical Sciences, Indian Institute of Science and Education Research (IISER), Sector 81, Mohali, Punjab 140306, India

furans synthesis when using biomass [15, 18–20]. The lower abundance of xylose in lignocellulose (nearly 20–25 wt%) restricts its preference in large-scale furfural production. But glucose is a more appealing biomass-derived carbohydrate because it is a less expensive and nature's most abundant monosaccharide. However, converting glucose into HMF is challenging when compared to fructose as a substrate due to its less reactivity [16].

Till date, numerous studies have demonstrated the selective formation of HMF (yield < 10%) and furfural (yield < 70%) using glucose and fructose [16, 21–25]. However, to the best of our knowledge, studies rarely focus on the one-pot selective synthesis of both HMF and furfural using glucose (as data shown in Table S2, SI). Moreover, many preferred the heterogeneous catalysis method for fructose/glucose dehydration, except for the report of Yu and co-workers, who employed the $SnSO_4/H_2SO_4$-based homogenous catalyst [23]. For instance, Li *et al.* developed the solid Brønsted acid catalyst by employing a multi-step copolymerization of paraformaldehyde and *p*-toluenesulfonic acid (*p*-TSA) technique and evaluated in furfurals synthesis using glucose [24]. It achieved only 14.6% HMF and 22.3% furfural in γ-valerolactone/water at 180 °C. Another study employing the Sn-beta zeolite exhibiting a higher number of Lewis acid (LA) sites reported a predominantly HMF (~ 60%) formation using glucose under similar operating conditions [25]. Many of the *p*-TSA catalyzed glucose conversion reactions determined that the specific product formation, either HMF or levulinic acid, is dependent on the catalytic conditions and the number of Lewis acidic sites [26–28]. For instance, Xu and co-workers reported enhanced glucose to levulinic acid conversion (up to 52% yield) over sulfonated carbon catalyst developed using *p*-TSA precursor at 170 °C under hydrothermal conditions [26]. Zhao and co-workers demonstrated the proficiency of *p*-TSA in homogenous glucose catalysis to HMF yielding up to 35% under similar conditions [27]. The study also attempted to increase the yield by modifying the system with the addition of chloride salts (such as $CrCl_3{\cdot}6H_2O$, $AlCl_3$, $FeCl_3{\cdot}6H_2O$, $FeCl_2{\cdot}2H_2O$, $ZnCl_2$, $CaCl_2$, $BaCl_2{\cdot}2H_2O$, $CuCl_2{\cdot}2H_2O$, $CoCl_2$, $MgCl_2{\cdot}2H_2O$, $NiCl_2{\cdot}6H_2O$, and H_3BO_3) behaving as Lewis acids, however, resulted in a substantial reduction in HMF yield. In exceptions, NH_4Cl resulted in a 13% improvement in HMF, which was attributed to its ammoniac characteristics, *i.e.,* the strong conjugate acid of the weak base ammonia. In another study, Wang et al. reported augmented furfural (50% yield and selectivity) and HMF (80% yield and 83% selectivity) production using fructose over H-β zeolite catalyst in γ-butyrolactone (GBL)/*N*-methyl pyrrolidone (NMP) solvents medium at 150 °C [29]. Literature reviews indicate that the noble metal-based catalysis of glucose to HMF or furfural is commonly preferred. Zhao *et al.* evaluated a various noble and non-noble metal chlorides ($CrCl_2$, $CrCl_3$, $FeCl_2$, $FeCl_3$, CuCl, $CuCl_2$, VCl_3, $MoCl_3$, $PdCl_2$, $PtCl_2$, $PtCl_4$, $RuCl_3$, or $RhCl_3$) for their potential on the synthesis of HMF using glucose in an ionic liquid [30]. Of all, the $CrCl_2$ (non-noble metal) enabled the highest HMF yield (70%), while the noble metal chlorides such as Pd and Pt reported a nearly 4–7% yield. In another study, Mondal and co-workers employed the 2% Pd–ZrO_2 nanocomposite for HMF using glucose and reported a 55% glucose conversion and 74% HMF selectivity at 160 °C [31]. However, the catalytic systems contain a high boiling point solvent and noble metal catalyst, which reduces the large-scale processing feasibility. A few studies have demonstrated a significant impact of the solvent medium on the selective synthesis of furfural and HMF chemicals [24, 25, 27, 29].

However, these chemicals are formed by different mechanisms when a glucose source is used. Glucose undergoes a two-step decomposition mechanism, *i.e.,* glucose to fructose isomerization, which is a straightforward step followed by dehydration, whereas fructose dehydration to furfural or HMF accommodates the synthesis of different intermediates. A fructose dehydration reaction ultimately delivers HMF; contrarily, the furfural synthesis involves a selective breaking of the C–C bond. Krishnan and co-workers conducted a mechanistic study to verify the pathway of fructose to HMF in water over boron-doped graphitic carbon nitride (*g*-CN) [32]. Cui and co-workers substantiated the plausible C–C bond cleavage mechanism of fructose to form furfural, which is promoted by the synergic effect of both GBL-Water and Hβ-zeolites [33]. All these reports suggest that the manipulation of the synergistic effect of acidic sites and solvents is critical to the selective synthesis of HMF and furfural using glucose or fructose.

In the past, various functionalized or metal-supported carbonaceous materials, such as graphene oxide, carbon nanotube, *g*-CN, carbon sphere, and activated carbon, have been exploited as heterogeneous catalysts for various organic transformations because of their cheap and easily available characteristics [34–38]. In recent years, the interest in exploring the applicability of the new class of low-cost carbon nanomaterial, *i.e.,* photoluminescent carbon dots (CD) has increased among scientists because of its wide range of potential applications, including nanotherapeutics, [39] bioimaging, [40] sonocatalysis, [41] energy storage, [42] electronics, [43] and organic transformation reactions [44]. Moreover, it possesses low toxicity, high surface area, good stability, and strong quantum confinement properties. Also, it can be readily prepared compared to other macroscopic carbonaceous materials [45]. From the recent studies, the renewable biomass resources can be utilized for its preparation, thereby establishing a value addition to the biomass and feasibility for large-scale production of catalytic chemicals production. For the synthesis of HMF using glucose/fructose, the sulfonated

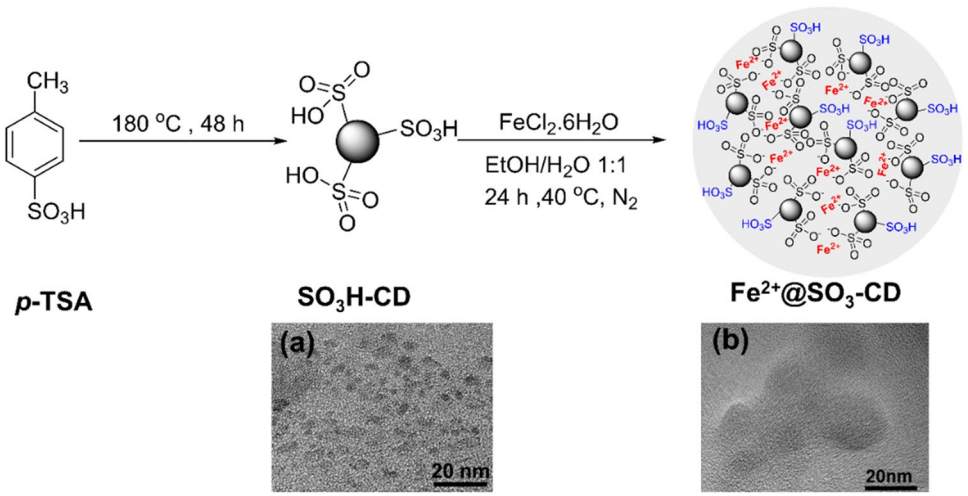

Scheme 1 Synthesis of SO_3H-functionalized CD (**SO_3H-CD**) and a further impregnation with iron (**Fe^{2+}@SO_3-CD**) and their TEM images

other carbon-based materials, such as carbon spheres, dendrimer, *g*-CN, biochar, and propyl sulfonate-functionalized magnetic graphene oxide nanocomposites are reported to be prominent [46–51]. However, the conversion follows a two-step strategy and, regrettably, involves harsh chemicals.

We have recently demonstrated a method for simple one-step preparation of sulfonic acid functionalized CD using a cheaper *p*-TSA precursor. The protocol involved no solvent usage and interestingly, the catalyst exhibited effectiveness in glucose conversion [44]. The catalyst exposing the Brønsted acid (BA) sites established by the -SO_3H groups outperformed the glucose dehydration to HMF and levulinic acid esterification to alkyl levulinate reactions. With the benefits of better catalytic efficiency and facile preparation, the present study was devoted to developing a multi-functional catalyst (*i.e.,* exposing both the Lewis and Brønsted acid sites) by impregnating the iron metal with the sulfonic acid attached to the CD to further improve the glucose conversion to furfurals (HMF and furfural). The resultant **Fe^{2+}@SO_3-CD** entailing a sturdy ionic interaction between Fe and -SO_3H can influence the glucose decomposition reaction under milder conditions. The characteristic Fe as a dopant can readily coordinate with the -SO_3H groups of CD, settle at the outer periphery and provide the Lewis acidic sites effective for the isomerization of glucose to fructose (which is a rate-determining step). In support, Zhang *et al.* attained a similar ionic interaction between Fe_2O_3 and -SO_3^- and reported a higher catalytic activity for the decomposition of H_2O_2 to hydroxyl radicals [52]. Thus, the novel **Fe^{2+}@SO_3-CD** can influence the selective synthesis of both furfural and HMF using glucose in a biphasic system (THF/H_2O); in this way, the catalytic setup may offer a synergistic effect to accelerate the reaction. The early version of the manuscript is available at ChemRxiv [53].

2 Experimental

2.1 Materials

All chemicals were purchased as analytical grade and used without any purifications. *p*-toluenesulfonic acid (*p*-TSA) was supplied by TCI Chemicals, Japan. Glucose, fructose, 5-hydroxymethylfurfural (HMF), furfural, $FeCl_2.6H_2O$, and absolute ethanol (EtOH) chemicals were supplied by Sigma-Aldrich chemicals. Organic solvents, such as tetrahydrofuran (THF), *N*-methyl-2-pyrrolidone (NMP), dimethyl sulfoxide (DMSO), dimethylformamide (DMF), 1-butanol (BuOH), and HPLC grade acetonitrile (CH_3CN), were purchased from Merck chemicals. The deionized (DI) water (H_2O) used for all sample preparations and dilutions was obtained using the Merck-Millipore water purifier system.

2.2 Synthesis of the dual acids functionalized carbon dot nanocomposite (Fe^{2+}@SO_3-CD)

A two-step protocol was followed for the preparation of carbon dot-sulfonic-iron (II) nanocomposite (**Fe^{2+}@SO_3-CD**) to expose both LA and BA sites. Briefly, first, the sulfonated acid-functionalized carbon dot (**SO_3H-CD**) was synthesized using the low-cost, and benchtop chemical *p*-TSA [44]. Second, the iron metal was impregnated into **SO_3H-CD**. Thereafter, 1 g **SO_3H-CD** was dispersed in 50 mL 1:1 EtOH/DI H_2O *v/v* under sonication for 10 min. Subsequently, 0.25 g $FeCl_2.6H_2O$ was added to the solution and stirred continuously for 24 h at 40 °C under N_2 atmosphere. The solid was then recovered through a high-speed centrifugation (10000 rpm for 20 min) and washed using DI water (3 × 10 mL). Finally, the solid residue was dried using a vacuum oven at 100 °C for 12 h to obtain a brown color powder (1.05 g) and labeled as **Fe^{2+}@SO_3-CD** nanocomposite. The synthesis scheme of **Fe^{2+}@SO_3-CD** is shown in Scheme 1.

2.3 Characterization Techniques

The attenuated total reflection-Fourier transform infrared (ATR-FTIR) spectra of the as-synthesized **Fe^{2+}@SO_3-CD** and **SO_3H-CD** were obtained using an FTIR instrument (Agilent Cary 660) in the range of $4000-400\ cm^{-1}$. The absorption spectra were recorded on a Shimadzu UV–vis spectrophotometer in 1 mL quartz cuvettes with a path length of 1 cm in THF solvent. The powder X-ray diffraction (P-XRD) spectroscopy was performed using a Bruker D8 Advance diffractometer in the 2θ range of $10-80°$. The transmission electron microscopic (TEM) images were acquired on a JEOL 2100 HR operating at 200 kV. The samples were prepared by drop-casting the diluted suspension of nanocomposite on a 300 mesh TEM copper grid (Beeta Tech India Pvt. Ltd) followed by drying under a vacuum for 24 h. The elemental composition and the mapping were analyzed by field emission scanning electron microscopy and energy-dispersive X-ray spectroscopy (FE-SEM/EDX). Before analysis, the diluted suspension of nanocomposite was drop cast on a silicon wafer and dried under an IR lamp for 24 h. The atomic force microscopic (AFM) images were obtained from a Bruker Multimode 8 instrument by employing the tapping mode of the dispersed sample drop cast on a silicon wafer. The thermogravimetric analysis (TGA) was performed using a thermogravimetric analyzer (Perkin Elmer STA 8000) at an N_2 flow rate of 10 mL/min and a heating rate of 10 °C/min. The X-ray photoelectron spectroscopy (XPS) spectra were recorded using a PHI 5000 Versa Probe high-performance electron spectrometer, coupled with monochromatic Al-Kα radiation (1486.6 eV) operating at an accelerating X-ray power of 50 W and 15 kV. The sample was outgassed at 25 °C in a UHV chamber ($<5\times10^{-7}$ Pa) before the measurement. The iron metal concentration determination was made using the inductively coupled plasma-mass spectrometry (ICP-MS) instrument (Varian 715-ES ICP Optical emission spectrometer). For the analysis, 5 mg of catalyst was dispersed in 50 mL HNO_3 (ICP-MS grade). The NH_3-temperature programmed desorption (NH_3-TPD) was performed to determine the active acid sites of the catalyst using the BELCAT II instrument. For the measurement, ~ 55 mg catalyst was pretreated under the stream of helium at 573 K for 60 min at a 60 mL/min flow rate. The evolved NH_3 was analyzed using a TCD detector (ShimadzuGC-14A). The ^{13}C-nuclear magnetic resonance (^{13}C-NMR) spectra were acquired on a Bruker Avance-II 400 MHz spectrometer using D_2O solvent at 298 K.

2.4 Reaction Procedure and Product Analysis

The catalytic glucose degradation experiments were performed in a hydrothermal autoclave consisting of a teflon chamber. In this experiment, 100 mg glucose and 50 mg catalyst were dissolved in 15 mL THF/H_2O. The reaction was performed in a hot-air oven at the desired time and temperature. After reaction completion, the catalyst was separated from the reaction mixture via high-speed centrifugation. The collected post-reaction mixture was analyzed using a high-performance liquid chromatography instrument (Waters 1525 with Waters 2707 autosampler) equipped with refractive index (RI; Waters 2414) and photodiode array (PDA; Waters 2998) detectors. The column used was XBridge Amide (3.5 µm, 4.6 × 250 mm) analytical column for sugars analysis by using CH_3CN/H_2O (8:2 v/v) with 0.2% Et_3N eluent at 0.8 mL/min and 40 °C. Similarly, the Eclipse plus-C18 (4.6 × 250 mm, 5 µm, Agilent) column was used for 5-HMF and furfural determinations by using CH_3CN/H_2O (1:1 v/v) eluent at 0.8 mL/min and 35 °C. The concentration of glucose, fructose, HMF, and furfural in the reaction mixture was quantified by using the respective calibration curves constructed using the standard chemicals. The yield and selectivity of the product(s) were calculated by using the formulae given in SI (Eqns. S1-S3). Meanwhile, the recovered solid catalyst was thoroughly washed using ethanol and DI water 3 to 4 times, dried at 60 °C overnight, and reused in the reaction.

3 Results and discussion

3.1 Physicochemical characterization of the as-synthesized Fe^{2+}@SO_3-CD

Our recent work demonstrated that the sulfonated carbon dot (**SO_3H-CD**) is promising for HMF synthesis using glucose ascribed to its higher Brønsted acid sites [44]. For furfural synthesis, LA sites are favorable, based on the literature [23, 54, 55]. A model system developed by Tao *et al.* comprising $FeCl_2$ in ionic liquids representing a homogenous catalytic setup has promoted the synthesis of both furfural and HMF using cellulose and determined that the role of LA is significant [55]. Given that both the LA and BA favor the glucose transformation, we developed a novel **Fe^{2+}@SO_3-CD** heterogeneous catalyst by combining the **SO_3H-CD** (a cheap and less toxic catalyst) and abundant earth metal $FeCl_2$ to establish the Lewis and Brønsted acid environments at low cost for the selective synthesis of HMF and furfural using glucose. The employed two-step protocol for synthesizing **Fe^{2+}@SO_3-CD** comprising an initial sulfonation of CDs using *p*-TSA as a precursor followed by impregnation of iron (II) can have a structural alteration due to the molecular coordination by the active species, as proposed in Scheme 1.

During catalyst synthesis, a nearly 1.05 g **Fe^{2+}@SO_3-CD** with 84% conversion was achieved by using 1 g of **SO_3H-CD** and 0.25 g of $FeCl_2$ precursors. Furthermore, the protocol was represented as simple, cost-effective, and less toxic

when compared to the conventional sulfur-acid treatment [46]. The synthesized **SO_3H-CD** appeared to be black; upon impregnation of the iron metal, it was discolored to brown. A variety of analytical characterization techniques, including FTIR, UV–vis, P-XRD, TEM, FE-SEM/EDX, AFM, TGA, NH_3-TPD, ICP-MS, and XPS were employed to determine the structural configuration and physicochemical properties of **Fe^{2+}@SO_3-CD**. The Fe metal coordination with **SO_3H-CD** was verified by using FTIR analysis. The comparative spectra display a significant shift in the peaks of 1142 and 1017 cm^{-1} to 1133 and 993 cm^{-1}, respectively, which are the corresponding asymmetric and symmetric stretching frequencies of O = S = O (Fig. 1a) [56].

The distinct peak at 470 cm^{-1} corresponds to the Fe–O bond, affirming the Fe coordination with the sulfonate group in **Fe^{2+}@SO_3-CD**. This resulted in a shift in the stretching frequency of the C–S peak from 684 to 692 cm^{-1}. All these instances infer the interaction between iron metal and oxygen atoms leading to an O–H bond peak intensity reduction. The observed shallow intense broad peak of O–H at 3376 cm^{-1} can be correlated to the $–SO_3H$ group interaction with the Fe atom to an extent.

The comparative UV–vis spectra of **Fe^{2+}@SO_3-CD** (Fig. S1) and **SO_3H-CD** [44] highlight that the former has an additional absorption peak at 275 nm, which belongs to the ligand to metal charge-transfer interaction (LMCT), based on the study by Li et al., who reported a similar effect of LMCT at 250 nm when synthesizing the Fe and O–Si nanocomposite [57]. However, the redshift (25 nm) in the wavelength is likely caused by the prevalent sulfonate environment around the Fe–O bond in **Fe^{2+}@SO_3-CD**. The result also indicated the sturdy interaction between Fe metal and sulfonate ligand. The comparative P-XRD data of **Fe^{2+}@SO_3-CD** (Fig. 1b) and **SO_3H-CD** [44] evidenced that the less or no alteration in the sulfonated CD's original crystallinity (amorphous) structure in the **Fe^{2+}@SO_3-CD** can be influenced by the Fe impregnation, indicating a significant intervention of the ionic interaction between iron and oxygen.

Furthermore, the performed TEM analysis to determine the size and surface morphology of **Fe^{2+}@SO_3-CD** nanocomposite revealed that it is a spherical-shaped particle and has a ~20 nm size (Scheme 1b & Fig. 2). However, the **SO_3H-CD** measures only 5 nm size (from the previous report [44]). Perhaps the ionic interaction of Fe^{2+} with SO_3^- increased the particle size through the carbon dots cluster. The additional AFM analysis witnessed the bulky particle size (as shown in Fig. S2, SI). The XPS analysis determined the oxidation states of active metals along with the elemental composition of **Fe^{2+}@SO_3-CD** (Figure S3, SI). Fig. S3a shows the XPS survey of **Fe^{2+}@SO_3-CD**;

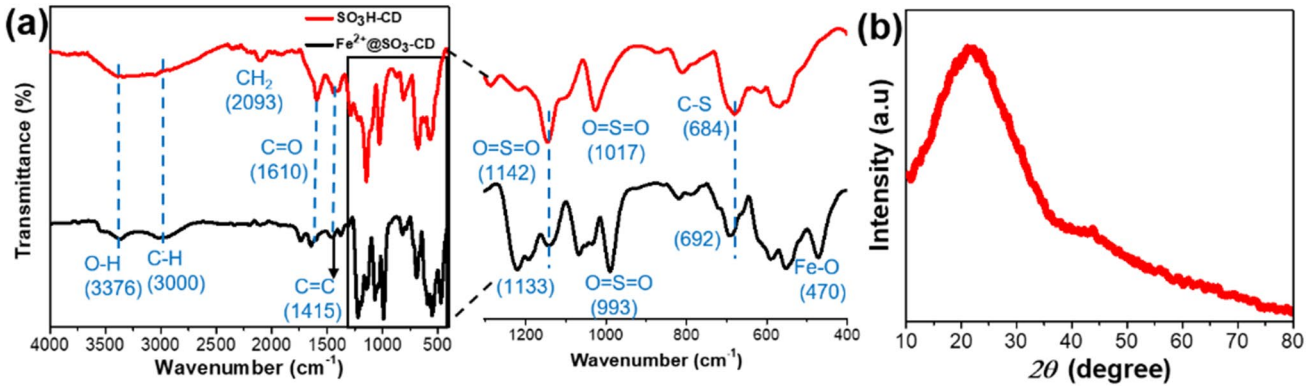

Fig. 1 (**a**) Comparative FT-IR result of as-synthesized **Fe^{2+}@SO_3-CD** and **SO_3H-CD** and (**b**) PXRD result of as-synthesized **Fe^{2+}@SO_3-CD**

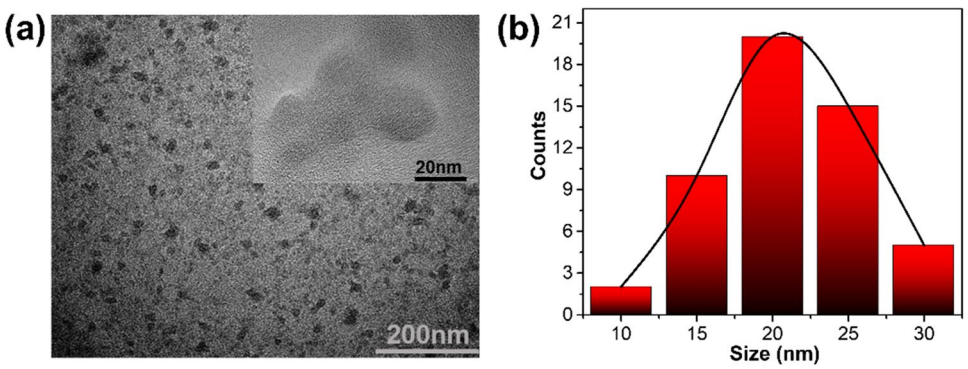

Fig. 2 (**a**) TEM image (Inset: zoomed image), (**b**) respective particle size distribution histogram of as-synthesized Fe^{2+}@SO_3-CD

it confirms the presence of carbon (C 1 s), oxygen (O 1 s), sulfur (S 2p), and iron (Fe 2p) photoelectrons. The deconvoluted XPS spectra for orbitals of Fe 2p, C 1 s, O 1 s, and S 2p of **Fe^{2+}@SO_3-CD** are present in Fig. S3b-e. In the O1s deconvoluted spectrum, an additional peak at 529.7 eV authenticates the Fe–O bond, which is absent in **SO_3H-CD** [44, 58]. The observed peaks at 531.6 and 530.6 eV were found to be common in **SO_3H-CD**, however, with an ~ 0.1 eV deviation [44]. Notably, a significant shift ~ 0.5 eV of C–S peak towards lower binding energy for O 1 s and S 2p was observed, articulating the formation of -SO_3-Fe^{2+} bond with charge-transfer interaction of iron metal and sulfonic acid functionalized CD [52]. The deconvoluted spectra of Fe^{II}2p display two peaks at binding energies of 710.4 eV and 724 eV correspond to the $Fe^{II}2p_{3/2}$ and $Fe^{II}2p_{1/2}$ states, respectively. The satellite peak at 714.79 eV was found in good agreement with the literature for the Fe^{2+}–O bond (Fig. S3b) [59]. The relative abundance of C, S, O, and Fe species and their mapping in the **Fe^{2+}@SO_3-CD** were determined via FE-SEM/EDX analysis. The results were found consistent with the findings of gravimetric analysis (as shown in Fig. S4 & S5, SI). Similarly, the quantitative determination of Fe content in the **Fe^{2+}@SO_3-CD** nanocomposite was made *via* ICP-MS analysis; the total Fe content was estimated to be 58.3 mg/g of catalyst by using the formulae (Eqn. S4, SI).

It is familiar that the catalytic performance of a solid catalyst is influenced by the thermal characteristics; therefore, the thermal stability of the catalyst was determined by using the TGA technique (Fig. S6). From the results, **Fe^{2+}@SO_3-CD** experienced a nearly 37% weight loss throughout the temperature range (*i.e.*, 800 °C), which is better than **SO_3H-CD**'s weight loss of 65% [44]. This expresses that the catalyst has higher thermal stability attributed to the prevalence of ionic interaction between Fe^{2+} and SO_3^-. While briefly discussing the trend of weight loss of the catalyst, it lost nearly 12% weight up to 450 °C, likely caused by the removal of surface adsorbed water molecules and Fe^{2+} and sulfonyl groups (to a small extent) [32]. A further increase in temperature up to 550 °C has influenced the catalyst's weight loss by 13%, which is due to the degradation of the unbounded SO_3H groups available at the surface periphery of the catalyst. Beyond and up to 750 °C, it attained a consistent weight loss of 14% because of the release of Fe^{2+} ions caused by the enhanced cleavage of the Fe–O bond. The presence of acidic sites in the catalyst is the key parameter for catalyzing the glucose isomerization and further conversion to HMF and furfural. Therefore, the NH_3-TPD analysis was performed to determine the total surface acidic sites (Fig. S7). The total surface acidity of the **Fe^{2+}@SO_3-CD** nanocomposite was estimated to be 1.687 mmol g^{-1}, which is comparatively higher than **SO_3H-CD** [44], which has 1.028 mmol g^{-1} total acidity. This increased total acidity of ~ 0.659 is due to the impregnation of Fe Lewis metal on sulfonated CDs. Overall, the analytical characterizations endorsed the catalytic ability of **Fe^{2+}@SO_3-CD**, at least, based on the exposure of different levels of acidic strengths, ascribed to the impregnation of Fe^{2+} ions into the sulfonic groups of CDs (Scheme 1), to promote the step-wise glucose transformation and higher temperature stability obligatory for the HMF and furfural preparation.

3.2 Fe^{2+}@SO_3-CD catalyzed glucose conversion

In anticipation, the fine-tuned dual acidic sites of **Fe^{2+}@SO_3-CD** nanocomposite can improve the selective synthesis of both HMF and furfural using glucose in a biphasic solvent system. Noteworthy that sugars have a higher dissolution capacity in water than organic solvents. However, the sugar catalysis towards HMF/furfural synthesis in water can undertake side reactions, resulting in levulinic acid, formic acid, and humin byproducts formation under the prevailing conditions. Therefore, the trend of supplementation of organic co-solvent as a reaction medium is popular to shield the HMF/furfural from further degradation and to develop a solvation shell around the carbohydrate molecule to enable a selective transformation. Initially, we verified the catalyst's ability on glucose decomposition in an appropriate biphasic medium. For this, the classical solvents, such as DMSO, DMF, 1-BuOH, NMP, and THF, were chosen as they are widely employed in combination with water to achieve higher biomass to product transformation [60–66]. The glucose conversion was carried out using 100 mg glucose, 100 mg catalyst, 120 °C, 5 h, and varying the 1:1 ratio of biphasic solvents; the corresponding results are present in Table S3, SI. Among the solvent systems, the THF/H_2O achieved the highest HMF/furfural yield (11%) through only 20% substrate consumption, which is much lower than the other systems utilizing up to 50% glucose. Suggesting that THF can control the unwanted glucose decomposition to unstructured humin [60, 61]. It is wise to use low boiling point solvents, like THF, which can help absorb water to strive the reaction forward and assist in the effortless recovery of products from the reaction mixture, thereby establishing a cost-effective process setup.

Having justified the preference of THF/H_2O as the reaction medium, the reaction's processing variables were subsequently optimized by following a conventional approach (*i.e.*, one factor at a time). The critical factors, such as temperature (from 120 to 160 °C), THF/H_2O ratio (from 1:0, 0:1, 2:1, 1:1, and 1:2 *v/v* ratio), time (from 5 to 19 h) and substrate/catalyst loading (from 1:0 to 3:1 *w/w* ratio), were selected for the optimization. The study on the effect of temperature disclosed that 140 °C is optimum to attain the maximum HMF formation (10%) after attaining a 39% glucose conversion (Fig. 3a). Further increase in temperature

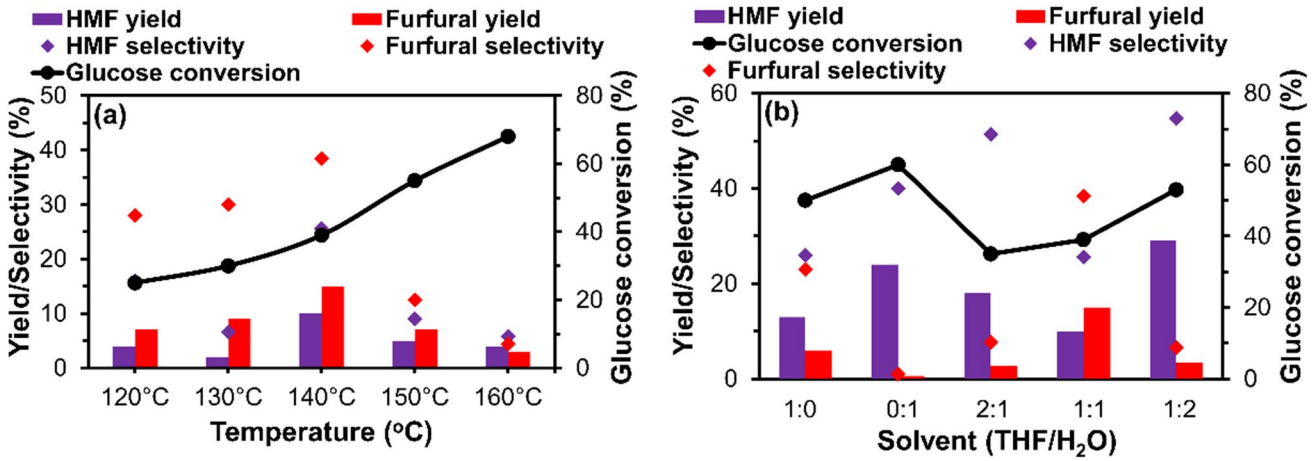

Fig. 3 Effect of (**a**) temperature at 1:1 THF/H_2O and (**b**) biphasic solvent at 140 °C combination on yield of HMF and furfural. Reaction conditions: 1:1 *w/w* ratio of glucose/catalyst, 5 h

resulted in higher conversion but with a lower yield of HMF/furfural due to an accelerated product degradation into undesirable compounds, specifically humin, as noticed by a change in color of the reaction mixture from light yellow to brown at higher temperatures [60, 61]. The optimized temperature. *i.e.,* 140 °C was kept constant for further studies. Thus, the THF/H_2O biphasic solvent represented an efficient catalytic system for glucose conversion. The ratio of THF/H_2O can have a significant influence on the yield and selectivity of both HMF and furfural. The solvent shell created on the substrate and catalyst may get affected by varying the aqueous and organic solvent ratio, which can drastically change the reaction outcome [67, 68]. The weak binding of water and THF to the Lewis iron metal center may get altered by the solvent ratio (1:1 THF/H_2O), affecting the outcome of the chemical reactivity [69]. Therefore, a different combination of THF/H_2O (1:0, 0:1, 2:1, 1:1, and 1:2 ratio) was evaluated by keeping the other parameters constant (Fig. 3b). The yield of HMF was found to be major in 0:1 and 1:2 THF/H_2O systems as 24 and 29%, respectively, while 1:0 and 2:1 THF/H_2O achieving relatively fewer yields as 13 and 18%, respectively. However, the 1:1 THF/H_2O system facilitated a furfural synthesis (15%) than HMF (10%). This could be likely due to the imbalance (2:1 and 1:2) of THF and water molecules leading to the suppression by blocking the iron metal active sites by interacting through oxygen atom present in both the solvents and preventing the pathway leading to furfural (*vide* infra.). Therefore, we considered the 1:1 and 1:2 THF/H_2O combinations as optimized conditions for furfural and HMF productions, respectively. Other parameters, *i.e.,* time and catalyst loading, were optimized to improve the yield further.

The effect of time (up to 19 h) on glucose conversion to HMF and furfural was studied in 1:2 and 1:1 THF/H_2O systems, respectively. We found that the optimum reaction times for maximum HMF (70%) and furfural (62%) formations were 15 and 9 h, respectively (Fig. 4). The results show that the prolonged reaction leads to a dramatic reduction in the yield, despite attainment of a relatively higher glucose conversion, indicating a further degradation of HMF and furfural into byproducts, specifically levulinic acid, formic acid, humin, etc. [61].

Lastly, the impact of catalyst amount on glucose, during HMF and furfural formation was studied. The glucose to catalyst ratio was changed from 1:1 to 3:1 by keeping other parameters constant (140 °C, 1:2, and 1:1 THF/H_2O, and 15 and 9 h as optimized conditions for HMF and furfural synthesis, respectively). Under this condition, we observed that when the catalyst loading is half of the glucose (Fig. 5), *i.e.*, 2:1 *w/w* ratio of glucose/catalyst, the system produced the highest yields of HMF (85%) and furfural (56%). Moreover, maximum selectivity was achieved at 94% (HMF) and 90% (furfural) under the optimized conditions with **Fe^{2+}@SO_3-CD**. This is accredited to the tunable characteristics of the THF/H_2O solvent system. The selectivity result is relatively higher than the literature for furfural/HMF synthesis using glucose or fructose (Table S2). For comparison, the reaction with no catalyst was performed at a 1:0 *w/w* ratio of glucose/catalyst and exhibited a > 80% glucose conversion, however, achieved a poor HMF and furfural yield. This implies the significance of catalyst in promoting the reaction as well as controlling the side reactions, including humin formation.

One of the merits of a solid-state heterogeneous catalytic system is the catalyst recoverability for reuse, which is beneficial for practical applications. Therefore, the **Fe^{2+}@SO_3-CD**'s reusability performance was evaluated. The catalyst allowed an effortless separation via formal high-speed centrifugation after each cycle. The catalyst was thoroughly washed to remove the residual product/reactant content using EtOH and DI H_2O (at least 3–4

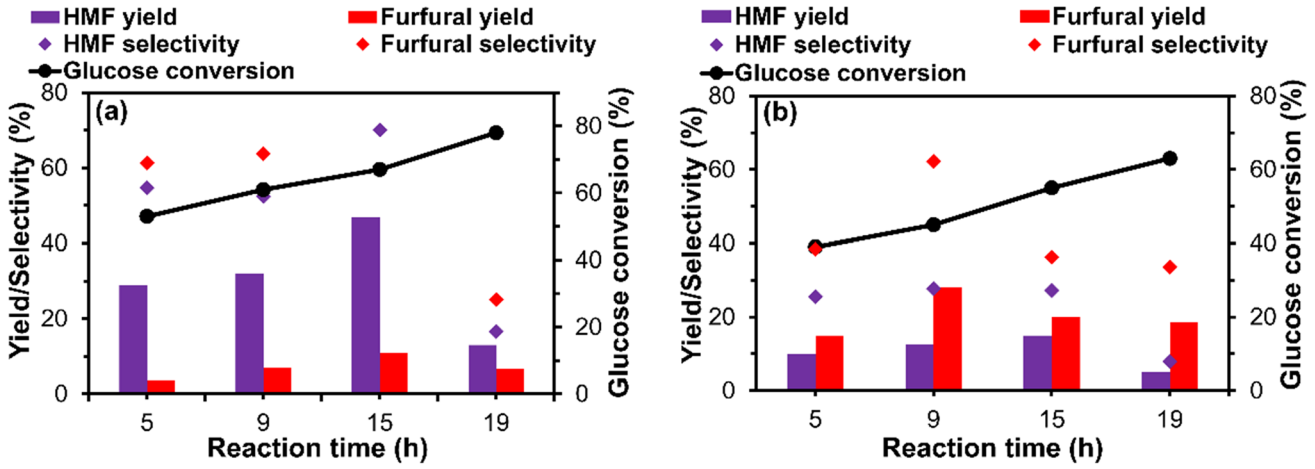

Fig. 4 Effect of time on conversion, yields, and selectivity of HMF and furfural using (**a**) 1:2 THF/H_2O and (**b**) 1:1 THF/H_2O. Reaction conditions: 1:1 *w/w* ratio of glucose/catalyst at 140 °C

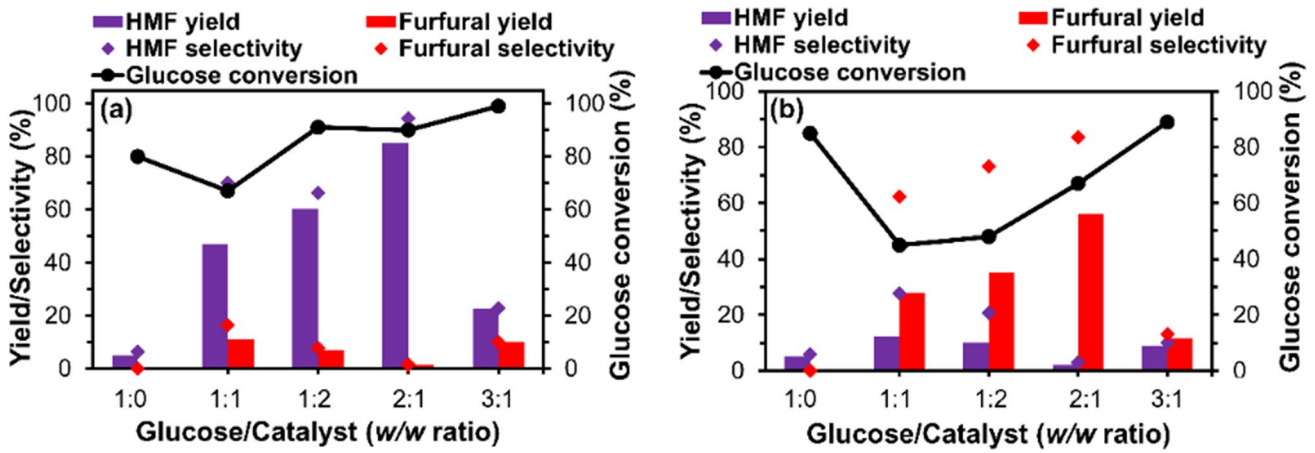

Fig. 5 Effect of catalyst loading on conversion, yields, and selectivity of HMF and furfural at 140 °C using (**a**) 1:2 THF/H_2O, 15 h, and (**b**) 1:1 THF/H_2O, 9 h

times) and dried at 60 °C overnight before reusing the catalyst. The results display that it shows effectiveness up to 4 cycles (Fig. S8, SI). In typical catalysis, the catalyst shows an activity reduction of up to 36% after the first cycle. This is due to the blockage of the catalyst's active sites by the formed humin that can stick to the catalyst surface [32]. But in our case, a slight reduction (5–8%) of yield in the case of both HMF (1:2 THF/H_2O) and furfural (1:1 THF/H_2O) after each cycle was noticed, implying that humin physical adsorption to the **Fe^{2+}@SO_3-CD** catalyst is minimum. The verification of the morphology and stability of the catalyst recovered after 4-cycles was made by running the XRD and TGA analysis. The comparative XRD spectra of fresh and reused catalysts display the least difference in the structural configuration (Fig. S9a, SI). Similarly, the stacked TGA graph of fresh and reused catalysts shows no significant change (particularly with the 1:2 THF/H_2O system). However, the catalyst belonging to the 1:1 THF/H_2O system suffered from a minor weight loss (Fig. S9b, SI)). This is likely caused due to the organic solvent weakening the iron coordination in the catalyst during catalysis at 140 °C multiple times and/or the produced side products (impurity) during the reaction deposited on the surface of the catalyst. This can be verified from the XRD results exhibiting additional minor peaks. Otherwise, the catalyst (of both 1:1 and 1:2 THF/H_2O systems) had a standard weight loss compared to the fresh catalyst up to 200 °C (Fig. S9b, SI). Additionally, the performed ICP-MS analysis disclosed that the catalyst (1:1 THF/H_2O system) lost nearly 19% Fe via metal leaching, while the other (1:2 THF/H_2O system) lost nearly 14% Fe. Overall, the catalyst offered the best performance for up to 4 recycles.

3.3 Plausible reaction mechanism of glucose reaction to furans over Fe^{2+}@SO_3-CD

Recently, Liu and Kerton determined that glucose/fructose conversion to fine chemicals strongly depends on the solvents' nature and the types of catalyst [70]. According to the literature, the Lewis and Brønsted acidic sites catalyzed mechanisms for the HMF synthesis using glucose generally follow two pathways: i) *via* fructose as an intermediate and/or ii) direct dehydration of glucose. In understanding, the Lewis metal, *i.e.,* Fe^{2+} can coordinate with the hydroxyl groups of C1 and C2, enabling the mutarotation and subsequent isomerization of glucose to yield fructose [30]. In this case, a parallel inhibition of the unpopular furfural, synthesis using glucose can be expected. Typically, its synthesis is achieved using fructose intermediate *via* sequential formation of arabinose (*via* C–C bond cleavage) and furfural through dehydration [23]. To unveil the mechanistic pathways of **Fe^{2+}@SO_3-CD** catalyzed glucose decomposition to HMF and furfural, We conducted the NMR study by using the intermittently collected reaction mixture performed under the optimum conditions (except for the time, which was kept at 5 h to ensure partial completion of the reaction to determine whether fructose forms as an intermediate). The ^{13}C NMR spectra of 1:2 THF/H_2O and 1:1 THF/H_2O systems are present in Fig. 6Aa and Ba, respectively. The comparison spectra of the reaction mixture and standard samples in Fig. 6A highlight the absence of fructose signals, but in Fig. 6B, the fructose signals can be seen. The results infer that the plausible mechanistic pathways for HMF are dependent on the water content (1:2 THF/H_2O), *i.e.,* direct dehydration of glucose to HMF through the BA activation pathway. Also, LA mediates the isomerization of glucose to fructose, followed by C–C cleavage for furfural synthesis (in a 1:1 THF/H_2O system) (Fig. 7).

To substantiate further, we performed the control studies using fructose as a feedstock over **Fe^{2+}@SO_3-CD** under the optimum conditions *i.e.,* 140 °C and 2:1 *w/w* ratio of fructose/catalyst in a 1:2 THF/H_2O system. It attained a maximum HMF formation of 95% with only 2% furfural (Table S4, SI). Contrarily, the reaction in 1:1 of THF/H_2O enabled a higher furfural formation (70%) than HMF (15%), indicating the influence of both solvents in promoting the multiple dehydration pathways. The results align with the sequential conversion strategy aided by **Fe^{2+}@SO_3-CD**; it is consistent with the hypothesis.

As a control, $FeCl_2$ was used as a catalyst for glucose conversion under the optimized conditions and found the formation of both furfural and HMF (Table S4, entries 5&6, SI). This infers that the furfural synthesis follows the LA pathway undertaking the isomerization of glucose to fructose followed by cleavage of fructose C–C bond and subsequent dehydration (Fig. 7). From the proposed mechanism, each pathway is influenced by both LA and BA sites. With the synergism between **Fe^{2+}@SO_3-CD** and THF/H_2O, for the formation of furfurals, the reaction progresses *via* the LA pathway in 1:1 ratio THF/H_2O and BA pathway, in 1:2 ratio THF/H_2O. From the reports, the BA functionalized solid-acid catalyst can generate both HMF and furfural using glucose at 14.2 and 22.3% yields, respectively, in γ-valerolactone/H_2O medium at 180 °C [24]. Thus, the remarkable glucose conversion and product(s) yield obtained by **Fe^{2+}@SO_3-CD** is accredited to balanced BA and LA sites. Therefore, the direct dehydration of glucose to HMF is quite possible in the 1:2 ratio THF/H_2O system with the least formation of fructose, which can rapidly undergo dehydration rather than other byproducts formation. This can also

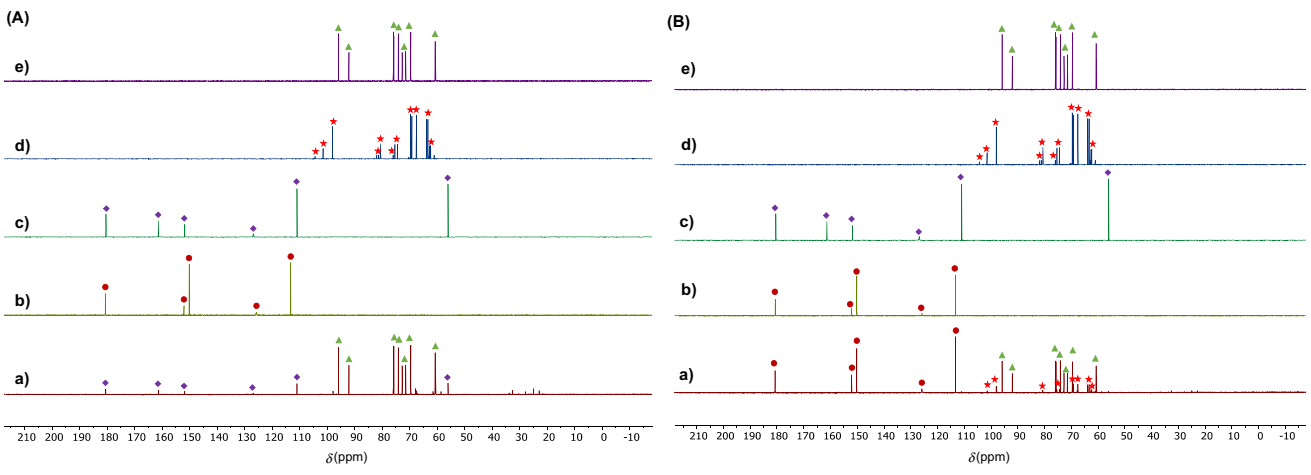

Fig. 6 Comparison of ^{13}C NMR spectra of partial (5 h) glucose conversion a) reaction mixture under the solvent conditions of (A) 1:2 THF/H_2O and (B) 1:1 THF/H_2O and standard samples of b) furfural, c) HMF, d) fructose, e) glucose

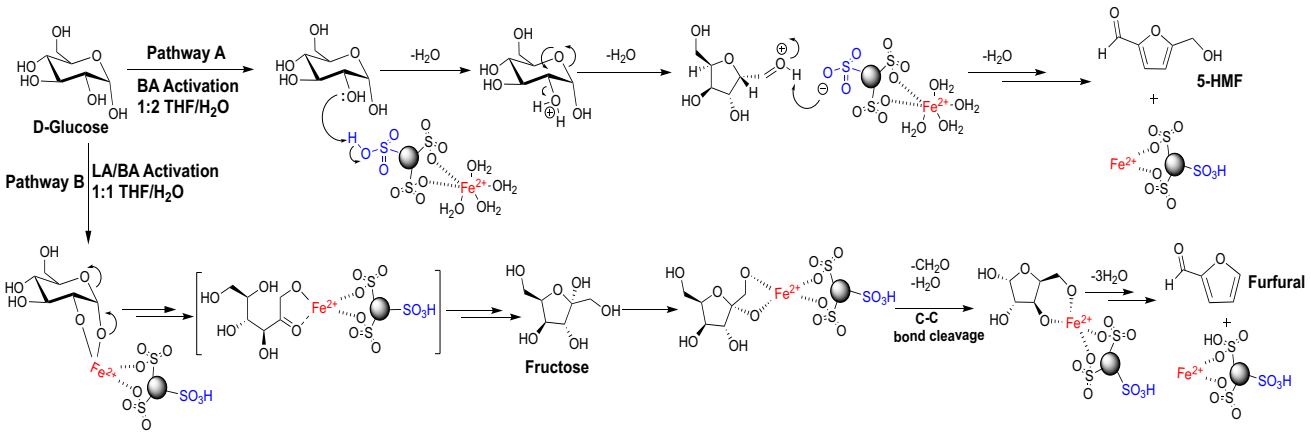

Fig. 7 The plausible mechanistic pathways of isomerization of glucose to fructose followed by dehydration of fructose to HMF and conversion of fructose to furfural

Table 1 Green metrics parameters for glucose to HMF and furfural synthesis under the conditions of 1:2 THF/H_2O, 15 h, and 1:1 THF/H_2O, 9 h, respectively at 2:1 *w/w* ratio of glucose/catalyst at 140 °C

S.No	Green metrics parameters	Calculated for HMF formation	Calculated for furfural formation
1	*E*-factor	0.563	2.224
2	Atom economy (%)	70	53.3
3	Reaction mass efficiency (%)	59.5	29.9
4	Carbon economy (%)	85.1	46.93
5	Mass productivity (%)	59.5	29.9
6	Mass intensity	1.67	3.335
7	Process mass intensity	1.563	3.224

be accounted for by the higher HMF formation in a 1:2 ratio THF/H_2O solvent system. Conversely, the 1:1 ratio THF/H_2O system can lead the reaction to form higher furfural *via* fructose and intermediate. Wherein, the Fe^{2+} center offering the Lewis acidic sites could trigger the fructose formation *via* the 1,2-hydride shift pathway. The resultant can be fully converted into furfural.

3.4 Green metrics and plausible mechanism

The economic and environmental sustainability of chemical reactions can be measured by the Green metrics factors [32, 71, 72]. The formulae used to calculate the green metrics parameters for the conversion of glucose into HMF and furfural are present in Eqns. S5–S11, SI, and the results are present in Table 1. The *E*-factor provides information on the efficiency of conversion of a waste (feedstock) to the desired product. In an ideal case, the *E*-factor lies between 0.42 and 0.72 if achieved 100% conversion for glucose to HMF and glucose to furfural, respectively. The *E*-factor value at the optimized conditions for HMF synthesis was found to be 0.52, while the furfural reaction was estimated at a 2.2 value. The *E*-factor value for HMF synthesis from glucose suggests that the **Fe^{2+}@SO_3-CD** catalyst is a sustainable material that can establish a greener strategy. The reaction's carbon economy was calculated to be > 85%, indicating that **Fe^{2+}@SO_3-CD** can facilitate a selective product formation (atom economy = 70%), *i.e.*, it can avoid undertaking the possible undesired side reactions. Overall, the setup established an environmentally friendly and economically viable method for mass production of furans (~ 60%). While for furfural synthesis, the *E*-factor value appears to be a bit higher than the theoretical range. Nevertheless, it can be regarded as a sustainable catalyst, based on the tunable catalyst's activity, limiting the unwanted side product(s) formation including humin, and controlling the glucose and product conversions. The possible reason for this high *E*-factor value could be the 38% non-conversion of glucose, which is also included as waste, but glucose would not harm the environment.

4 Conclusions

Due to the high cost and lower availability of noble metals, dedicated efforts are made in the design and development of highly selective, cheap, and stable non-noble metal catalytic systems to convert biomass-derived glucose into furfural and HMF platform chemicals under mild reaction conditions. Herein, we synthesized a sustainable and effective catalyst **Fe^{2+}@SO_3-CD** using iron metal as Lewis metal acid and sulfonic acid functionalized CDs as Brønsted acid precursors for the selective synthesis of HMF and furfural directly from glucose. The comprehensive characterizations of **Fe^{2+}@SO_3-CD** affirmed the successful

impregnation of Fe^{2+} with the SO_3^- group of CDs *via* ionic interaction. However, this resulted in three times bigger particle size than **SO_3H-CD** size, *i.e.*, ~ 20 nm size **Fe^{2+}@SO_3-CD**. Fascinatingly, the catalyst enabled an 85% HMF yield with a 1:2 THF/H_2O within 15 h with 94% selectivity. In a separate 1:1 THF/H_2O system, nearly 56% yield of furfural was achieved within 9 h with 90% selectivity. This is accredited to the synergic effect between **Fe^{2+}@SO_3-CD** and the biphasic (THF/H_2O) solvent system. While many reports have been published in recent years on the synthesis of HMF or furfural from glucose/xylose, to the best of our knowledge, the synthesis of both furfural and HMF using the single substrate over a multi-functional catalyst at a highly selective rate is a rare and novel approach. The detailed mechanistic investigation through NMR studies unveiled the Brønsted acid-mediated direct water dehydration pathway for the formation of HMF in a 1:2 THF/H_2O medium. Similarly, the LA-mediated pathway of glucose to fructose (as an intermediate) isomerization followed by C–C cleavage leads to the formation of furfural in the 1:1 THF/H_2O system. The catalyst was represented as a model to activate a higher selective synthesis of both furfural and HMF at 140 °C, which is a relatively lower temperature (Table S2), through control of humin and other side product formations. The catalytic system also contributed to furans' selective synthesis simply by tuning the water ratio. Thus, the discovery may offer new insights into the glucose decomposition mechanism and help in the design and development of a variety of non-noble metal catalytic systems for glucose transformation.

Supplementary Information The online version contains supplementary material available at https://doi.org/10.1007/s13399-022-03182-w.

Acknowledgements The authors thank the Department of Biotechnology (DBT) for the financial support for this work through the flagship program (Grant no. BT/CIAB-Flagship/2018). GJ thanks the Department of Science and Technology (DST) for the project grant (No. SB/S2/RJN-047/2015) and DST-SERB for the Ramanujan Fellowship.

Author contribution Raina Sharma contributed to methodology, validation, investigation and writing including review and editing; Abdul Selim performed investigation and writing including review and editing; Bhawana Devi, Senthil M Arumugam, and Shaifali Sartaliya carried out investigation; Sasikumar Elumalai performed supervision and writing including review and editing; Govindasamy Jayamurugan contributed to conceptualization, supervision, writing of the original draft, and writing including review and editing.

Declarations

Conflict of interest The early version of the manuscript is available at the ChemRxiv non-peer review platform at https://doi.org/10.26434/chemrxiv-2022-lx28n. The authors declare no competing financial interest.

References

1. Kramer GJ, Haigh M (2009) No quick switch to low-carbon energy. Nature 462:568–569
2. Martins F, Felgueiras C, Smitkova M, Caetano N (2019) Analysis of fossil fuel energy consumption and environmental impacts in European Countries. Energies 12:964
3. Bennich T, Belyazid S (2017) The route to sustainability—prospects and challenges of the bio-based economy. Sustainability 9:887
4. Cai J, He Y, Yu X, Banks SW, Yang Y, Zhang X, Yu Y, Liu R, Bridgwater AV (2017) Review of physicochemical properties and analytical characterization of lignocellulosic biomass. Renew Sustain Energy Rev 76:309–322
5. Mika LT, Cséfalvay E, Németh Á (2018) Catalytic conversion of carbohydrates to initial platform chemicals: chemistry and sustainability. Chem Rev 118:505–613
6. Fang W, Riisager A (2021) Recent advances in heterogeneous catalytic transfer hydrogenation/hydrogenolysis for valorization of biomass-derived furanic compounds. Green Chem 23:670–688
7. Van Putten R-J, Van der Waal JC, De Jong E, Rasrendra CB, Heeres HJ, De Vries JG (2013) Hydroxymethylfurfural A versatile platform chemical made from renewable resources. Chem Rev 113:1499–1597
8. Li Y, Bhagwat SS, Cortés-Peña YR, Ki D, Rao CV, Jin Y-S, Guest JS (2021) Sustainable lactic acid production from lignocellulosic biomass. ACS Sustain Chem Eng 9:1341–1351
9. Li Z, Zhu C, Wang H, Liang Y, Xin H, Li S, Hu X, Wang C, Zhang Q, Liu Q, Ma L (2021) 5-Hydroxymethylfurfural hydrodeoxygenation coupled with water-gas shift reaction for 2,5-Dimethylfuran production over Au/ZrO_2 catalysts. ACS Sustain Chem Eng 9:6355–6369
10. Liu H, Jia W, Yu X, Tang X, Zeng X, Sun Y, Lei T, Fang H, Li T, Lin L (2021) Vitamin C-Assisted synthesized Mn–Co Oxides with improved oxygen vacancy concentration: boosting lattice oxygen activity for the Air-Oxidation of 5-(Hydroxymethyl)Furfural. ACS Catal 11:7828–7844
11. Kucherov FA, Romashov LV, Galkin KI, Ananikov VP (2018) Chemical transformations of biomass-derived C_6-Furanic platform chemicals for sustainable energy research materials science and synthetic building blocks. ACS Sustain Chem Eng 6:8064–8092
12. Gallezot P (2012) Conversion of biomass to selected chemical products. Chem Soc Rev 41:1538–1558
13. Gérardy R, Debecker DP, Estager J, Luis P, Monbaliu J-CM (2020) Continuous flow upgrading of selected C_2–C_6 platform chemicals derived from biomass. Chem Rev 120:7219–7347
14. Xu C, Paone E, Rodríguez-Padrón D, Luque R, Mauriello F (2020) Recent catalytic routes for the preparation and the upgrading of biomass derived furfural and 5-Hydroxymethylfurfural. Chem Soc Rev 49:4273–4306
15. Wang Y, Yang X, Zheng H, Li X, Zhu Y, Li Y (2019) Mechanistic insights on catalytic conversion fructose to furfural on beta zeolite via selective carbon-carbon bond cleavage. Mol Catal 463:130–139
16. Cai CM, Zhang T, Kumar R, Wyman CE (2014) Integrated furfural production as a renewable fuel and chemical platform from lignocellulosic biomass. J Chem Technol Biotechnol 89:2–10
17. Verma S, Baig RN, Nadagouda MN, Len C, Varma RS (2017) Sustainable pathway to furanics from biomass via heterogeneous organo-catalysis. Green Chem 19:164–168
18. Svenningsen GS, Kumar R, Wyman CE, Christopher P (2018) Unifying mechanistic analysis of factors controlling selectivity in fructose dehydration to 5-hydroxymethylfurfural by homogeneous acid catalysts in aprotic solvents. ACS Catal 8:5591–5600

19. Zhang L, Xi G, Yu K, Yu H, Wang X (2017) Furfural production from biomass-derived carbohydrates and lignocellulosic residues via heterogeneous acid catalysts. Ind Crops Prod 98:68–75
20. Lacerda VDS, López-Sotelo JB, Correa-Guimarães A, Hernández-Navarro S, Sánchez-Bascones M, Navas-Gracia LM, Martín-Ramos P, Pérez-Lebeña E, Martín-Gil J (2015) A kinetic study on microwave-assisted conversion of cellulose and lignocellulosic waste into hydroxymethylfurfural/furfural. Bioresour Technol 180:88–96
21. Zhang L, Xi G, Chen Z, Jiang D, Yu H, Wang X (2017) Highly selective conversion of glucose into furfural over modified zeolites. Chem Eng J 307:868–876
22. Asakawa M, Shrotri A, Kobayashi H, Fukuoka A (2019) Solvent basicity controlled deformylation for the formation of furfural from glucose and fructose. Green Chem 21:6146–6153
23. Zhang Y, Wang P, Liu L, Wang Q, Yang N, Yu H (2021) Experimental and kinetic study on the production of furfural and HMF from glucose. Catalysts 11:11
24. Li W, Xu Z, Zhang T, Li G, Jameel H, Chang HM, Ma L (2016) Catalytic conversion of biomass-derived carbohydrates into 5-hydroxymethylfurfural using a strong solid acid catalyst in aqueous γ-valerolactone. BioResources 11:5839–5853
25. Zhang T, Fan W, Li W, Xu Z, Xin H, Su M, Lu Y, Ma L (2017) One-pot conversion of carbohydrates into HMF using heterogeneous Lewis and Brønsted Acid catalysts. Energy Technol 5:747–755
26. Kang S, Zhang G, Yang X, Yin H, Fu X, Liao J, Tu J, Huang X, Qin FG, Xu Y (2017) Effects of p-toluenesulfonic acid in the conversion of glucose for levulinic acid and sulfonated carbon production. Energy Fuels 31:2847–2854
27. Sajid M, Bai Y, Liu D, Zhao X (2021) Conversion of glucose to 5-Hydroxymethylfurfural by Co-catalysis of p-Toluenesulfonic Acid (pTSA) and chlorides: A comparison based on kinetic modeling. Waste Biomass Valori 12:3271–3286
28. Choudhary V, Mushrif SH, Ho C, Anderko A, Nikolakis V, Marinkovic NS, Frenkel AI, Sandler SI, Vlachos DG (2013) Insights into the interplay of Lewis and Brønsted acid catalysts in glucose and fructose conversion to 5-(hydroxymethyl) furfural and levulinic acid in aqueous media. J Am Chem Soc 135:3997–4006
29. Wang Y, Ding G, Yang X, Zheng H, Zhu Y, Li Y (2018) Selectively convert fructose to furfural or hydroxymethylfurfural on Beta zeolite: The manipulation of solvent effects. Appl Catal B: Environ 235:150–157
30. Zhao H, Holladay JE, Brown H, Zhang ZC (2007) Metal chlorides in ionic liquid solvents convert sugars to 5-hydroxymethylfurfural. Science 316:1597–1600
31. Goyal R, Abraham BM, Singh O, Sameer S, Bal R, Mondal P (2022) One-pot transformation of glucose into hydroxymethyl furfural in water over Pd decorated acidic ZrO2. Renew Energy 183:791–801
32. Chhabra T, Dhingra S, Nagaraja CM, Krishnan V (2021) Influence of Lewis and Brønsted acidic sites on graphitic carbon nitride catalyst for aqueous phase conversion of biomass-derived monosaccharides to 5-hydroxymethylfurfural. Carbon 183:984–998
33. Cui J, Tan J, Deng T, Cui X, Zhu Y, Li Y (2016) Conversion of carbohydrates to furfural via selective cleavage of the carbon–carbon bond: the cooperative effects of zeolite and solvent. Green Chem 18:1619–1624
34. Bahuguna A, Kumar A, Krishnan V (2019) Carbon-support-based heterogeneous nanocatalysts: synthesis and applications in organic reactions. Asian J Org Chem 8:1263–1305
35. Kuang Y, Li H (2021) Targeted engineering of metal@ hollow carbon spheres as nanoreactors for biomass hydrodeoxygenation. Renew Sust Energ Rev 151:111582
36. Huang H, Zong R, Li H (2020) Synergy effects between oxygen groups and defects in hydrodeoxygenation of biomass over a carbon nanosphere supported Pd catalyst. ACS Sustain Chem Eng 8:15998–16009
37. Li T, Li H, Li C (2022) Hydrodeoxygenation of vanillin to creosol under mild conditions over carbon nanospheres supported palladium catalysts: Influence of the carbon defects on surface of catalysts. Fuel 310:122432
38. Chhabra T, Rohilla J, Krishnan V (2022) Nanoarchitectonics of phosphomolybdic acid supported on activated charcoal for selective conversion of furfuryl alcohol and levulinic acid to alkyl levulinates. Mol Catal 519:112135
39. Zheng M, Liu S, Li J, Qu D, Zhao H, Guan X, Hu X, Xie Z, Jing X, Sun Z (2014) Integrating oxaliplatin with highly luminescent carbon dots: an unprecedented theranostic agent for personalized medicine. Adv Mater 6:3554–3560
40. Yang S-T, Cao L, Luo PG, Lu F, Wang X, Wang H, Meziani MJ, Liu Y, Qi G, Sun Y-P (2009) Carbon dots for optical imaging in vivo. J Am Chem Soc 131:11308–11309
41. Selim A, Kaur S, Dar AH, Sartaliya S, Jayamurugan G (2020) Synergistic effects of carbon dots and palladium nanoparticles enhance the Sonocatalytic performance for Rhodamine B degradation in the absence of light. ACS Omega 5:22603–22613
42. Li L, Li Y, Ye Y, Guo R, Wang A, Zou G, Hou H, Ji X (2021) Kilogram-scale synthesis and functionalization of carbon dots for superior electrochemical potassium storage. ACS Nano 15:6872–6885
43. Semeniuk M, Yi Z, Poursorkhabi V, Tjong J, Jaffer S, Lu Z-H, Sain M (2019) Future perspectives and review on organic carbon dots in electronic applications. ACS Nano 13:6224–6255
44. Selim A, Sharma R, Arumugam SM, Elumalai S, Jayamurugan G (2022) Sulphonated carbon dots synthesized through a one-pot facile and scalable protocol facilitates the preparation of renewable precursors using glucose/levulinic acid. ChemistrySelect 7:e202104448
45. Liu J, Li R, Yang B (2020) Carbon dots: a new type of carbon-based nanomaterial with wide applications. ACS Cent Sci 6:2179–2195
46. Zhao J, Zhou C, He C, Dai Y, Jia X, Yang Y (2016) Efficient dehydration of fructose to 5-hydroxymethylfurfural over sulfonated carbon sphere solid acid catalysts. Catal 264:123–130
47. Karimi S, Seidi F, Niakan M, Shekaari H, Masteri-Farahani M (2021) Catalytic dehydration of fructose into 5-hydroxymethylfurfural by propyl sulfonic acid functionalized magnetic graphene oxide nanocomposite. Renew Energy 180:132–139
48. Sun S, Zhao L, Yang J, Wang X, Qin X, Qi X, Shen F (2020) Eco-friendly synthesis of SO_3H-containing solid acid via mechanochemistry for the conversion of carbohydrates to 5-hydroxymethylfurfural. ACS Sustain Chem Eng 8:7059–7067
49. Niakan M, Masteri-Farahani M, Karimi S, Shekaari H (2022) Sulfonic acid functionalized dendrimer-grafted cellulose as a solid acid catalyst for the high-yield and green production of 5-hydroxymethylfurfural. Sustain Energy Fuels 6:2514–2522
50. Chhabra T, Bahuguna A, Dhankhar SS, Nagaraja CM, Krishnan V (2019) Sulfonated graphitic carbon nitride as a highly selective and efficient heterogeneous catalyst for the conversion of biomass-derived saccharides to 5-hydroxymethylfurfural in green solvents. Green Chem 21:6012–6026
51. Kumari N, Chhabra T, Kumar S, Krishnan V (2022) Nanoarchitectonics of sulfonated biochar from pine needles as catalyst for conversion of biomass derived chemicals to value added products. Catal Commun 168:106467
52. Zhang G, Qin L, Wu Y, Xu Z, Guo X (2015) Iron oxide nanoparticles immobilized to mesoporous NH_2-SiO_2 spheres by sulfonic

acid functionalization as highly efficient catalysts. Nanoscale 7:1102–1109
53. Sharma R, Selim A, Devi B, Murugan SR, Sartaliya S, Elumalai S, Jayamurugan G (2022) Realizing direct conversion of glucose to furfurals with tunable selectivity utilizing a carbon dot catalyst with dual acids controlled by a biphasic medium. ChemRxiv. https://doi.org/10.26434/chemrxiv-2022-lx28n
54. Zhang Z, Zhao ZK (2010) Microwave-assisted conversion of lignocellulosic biomass into furans in ionic liquid. Bioresour Technol 101:1111–1114
55. Tao F, Song H, Chou L (2010) Hydrolysis of cellulose by using catalytic amounts of $FeCl_2$ in ionic liquids. Chemsuschem 3:1298–1303
56. Nakajima K, Hara M (2012) Amorphous carbon with SO_3H groups as a solid Brønsted Acid catalyst. ACS Catal 2:1296–1304
57. Li C (2003) Identifying the isolated transition metal ions/oxides in molecular sieves and on oxide supports by UV resonance Raman spectroscopy. J Catal 216:203–212
58. Li L, Ma P, Hussain S, Jia L, Lin D, Yin X, Lin Y, Cheng Z, Wang L (2019) FeS_2/carbon hybrids on carbon cloth: a highly efficient and stable counter electrode for dye-sensitized solar cells. Sustain Energy Fuels 3:1749–1756
59. Shaw SK, Alla SK, Meena SS, Mandal RK, Prasad NK (2017) Stabilization of temperature during magnetic hyperthermia by Ce substituted magnetite nanoparticles. J Magn Magn Mater 434:181–186
60. Nahavandi M, Kasanneni T, Yuan ZS, Xu CC, Rohani S (2019) Efficient conversion of glucose into 5-Hydroxymethylfurfural using a sulfonated carbon-based solid acid catalyst: an experimental and numerical study. ACS Sustain Chem Eng 7:11970–11984
61. Steinbach D, Kruse A, Sauer J (2017) Pretreatment technologies of lignocellulosic biomass in water in view of furfural and 5-hydroxymethylfurfural production- A review. Biomass Conv Bioref 7:247–274
62. Nikolla E, Roman-Leshkov Y, Moliner M, Davis ME (2011) ″One-Pot″ synthesis of 5-(Hydroxymethyl)Furfural from carbohydrates using Tin-Beta Zeolite. ACS Catal 1:408–410
63. Agirrezabal-Telleria I, Gandarias I, Arias PL (2014) Heterogeneous acid catalysts for the production of furan-derived compounds (furfural and hydroxymethylfurfural) from renewable carbohydrates: A review. Catal Today 234:42–58
64. Zhao Y, Lu K, Xu H, Zhu L, Wang S (2021) A critical review of recent advances in the production of furfural and 5-hydroxymethylfurfural from lignocellulosic biomass through homogeneous catalytic hydrothermal conversion. Renew Sustain Energy Rev 139:110706
65. Kucherov FA, Galkin KI, Gordeev EG, Ananikov VP (2017) Efficient route for the construction of polycyclic systems from bioderived HMF. Green Chem 19:4858–4864
66. Ricciardi LL, Verboom W, Lange J-P, Huskens J (2022) Production of furans from C5 and C6 sugars in the presence of polar organic solvents. Sustain Energy Fuels 6:11–28
67. Li J, Zhang W, Xu S, Hu C (2020) The roles of H_2O/tetrahydrofuran system in lignocellulose valorization. Front Chem 8:70
68. Wrigstedt P, Keskiväli J, Leskelä M, Repo T (2015) The role of salts and Brønsted acids in Lewis Acid-Catalyzed aqueous-phase glucose dehydration to 5-Hydroxymethylfurfural. ChemCatChem 7:501–507
69. Kumar A, Blakemore JD (2021) On the use of aqueous Metal-Aqua pKa values as a descriptor of Lewis acidity. Inorg Chem 60:1107–1115
70. Liu Y, Kerton FM (2021) Mechanistic studies on the formation of 5-hydroxymethylfurfural from the sugars fructose and glucose. Pure Appl Chem 93:463–478
71. Sheldon R (2018) A Metrics of green chemistry and sustainability: past present and future. ACS Sustain Chem Eng 6:32–48
72. Chhabra T, Dwivedi P, Krishnan V (2022) Acid functionalized hydrochar as heterogeneous catalysts for solventless synthesis of biofuel precursors. Green Chem 24:898–910